Topology-Optimized Spatially Modulated PVGs for Uniform Exit Pupil Expansion in AR Waveguide Displays

Wanchen Zhang[1], Yishi Weng*, Liang Zhou , Chuang Wang , Ran Wei, Nan Lin and Yuning Zhang

*yishi@seu.edu.cn
[1] Joint International Research Laboratory of Information Display and Visualization
School of Electronic Science and Engineering, Southeast University, Nanjing, Jiangsu 210096, China
Keywords: Polarization volume grating; Diffracted waveguide display; Uniformity; AR display.

ABSTRACT

This paper presents a partition uniformity optimization method based on polarization beam grating (PVG). By adjusting the grating partition width of the coupling area to form blank areas, the uniformity is optimized. The results show that the uniformity of the exit pupil has significantly improved, and the uniformity of the FOV within the eyebox has increased by nearly twice.

1 Introduction

In recent years, diffractive waveguides have emerged as a focal point in optical display research, driven by the rapid development of near-eye display technologies like augmented reality (AR) and head-mounted displays (HMD)[1-2]. Among these, surface relief gratings (SRG) enable light diffraction control through precise micro-nano processing but suffer from complex fabrication and high costs. Volume holographic gratings (VHG) achieve high diffraction efficiency by recording interference fringes in holographic materials, yet their optical performance is vulnerable to environmental fluctuations. The polarization volume holographic waveguide (PVG) technology, however, integrates the merits of polarization optics and volume holography, optimizing optical performance while reducing system complexity.

Despite its promise, PVG technology is challenged by poor exit pupil uniformity and inefficient regulation[3]. Minor eye or head movements can lead to significant brightness disparities across the field of view, exacerbating visual fatigue in binocular systems. Moreover, the growing demand for two-dimensional pupil expansion in waveguide technology presents a trade-off[4]: increasing the expansion area dilutes light intensity per unit area, reducing perceived brightness with fixed total light energy.

Previous studies have explored diffraction efficiency regulation. Ding et al. enhanced uniformity by 2.3 times at a 50° field of view by optimizing PVG thickness and tilt angle to meet the first-order half-wave condition[5]. Lee et al. highlighted the critical role of grating thickness in PVG diffraction efficiency[6]. Yang Hui et al. proposed a metasurface-based design for large-angle uniform diffraction gratings, improving diffraction efficiency by 8.3% via propagation phase regulation and equivalent medium theory[7].

This study proposes a polarization volume holographic waveguide with controllable regional efficiency. By leveraging differential diffraction properties across grating regions and total internal reflection (TIR) in non-grating areas, it minimizes optical energy loss and ensures uniform illumination.

2 Influence of diffraction efficiency on uniformity

The three-dimensional spiral periodic physical structure of PVG is shown in Fig. 1. Light beams enter the grating in the x-plane, where elliptical objects represent liquid crystal molecules, with their aspect ratios indicating different angles of periodic spiral rotation inside the grating. As the main material, liquid crystal molecules rotate periodically in the grating's three-dimensional space. The period in the x-direction is tuned by adjusting the exposure angles of two coherent beams in holographic exposure, while the period in the y-direction is modulated by the concentration of chiral materials based on their helix twist power (HTP).

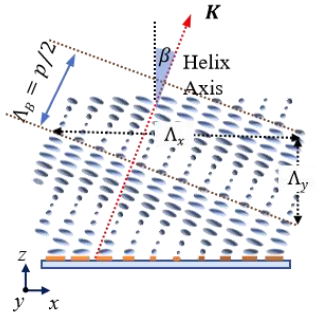

Fig. 1 Schematic diagrams of PVG structures.

When the PVG grating structure reaches a sufficient thickness, efficient volume grating diffraction can be achieved, and the Bragg condition is expressed as:

$$2\Lambda_B n_{eff} \cos\varphi = \lambda_B \tag{2.1}$$

According to geometric relations, the relationships among the grating transverse period Λ_x, longitudinal period Λ_y, and Bragg diffraction period Λ_B are as follows:

$$\begin{cases} \Lambda_x = \Lambda_B / sin\beta \\ \Lambda_y = \Lambda_B / cos\beta \end{cases} \tag{2.2}$$

Only when the incident angle and wavelength of light

satisfy the Bragg condition can PVG achieve efficient single-order diffraction, so differences in grating structure parameters directly affect PVG's diffraction efficiency.

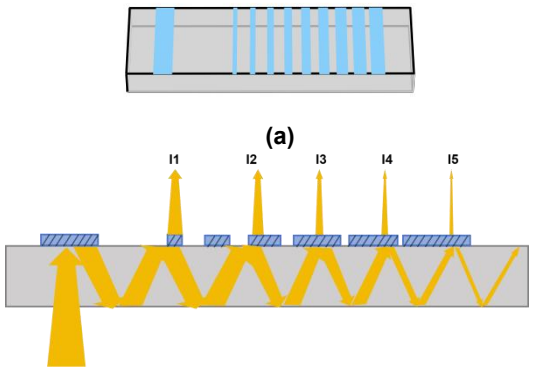

Fig.2 (a) Schematic of PVG structure with zonal efficiency regulation, (b) Schematic of exit light energy distribution at waveguide exit pupil after efficiency regulation.

After light is diffracted into the waveguide by the input coupler grating, total internal reflection (TIR) is used to complete exit pupil replication and expansion. However, cumulative diffractive intensity loss causes gradual brightness decay, affecting full-field brightness uniformity. To leverage PVG's high efficiency from single-order diffraction, our team performed zonal regulation on the diffraction efficiency of PVG out-coupling grating structures. As shown in Fig. 2(a), adjustable-width strip non-grating regions with gradient distribution along the light propagation direction are formed on the out-coupling grating. During TIR propagation in the waveguide, grating regions diffract light out, while non-grating regions maintain TIR, minimizing energy waste by reducing diffraction in non-grating areas. Based on the above principle, continuous and uniform imaging is achieved by adjusting the duty cycle and period. Each sub-period consists of a grating region and a non-grating region, where the duty cycle denotes the proportion of the grating region in the sub-period, and the period is composed of one grating region and one non-grating region.As shown in Fig. 2(b), energy, via total internal reflection in non-grating regions, enhances full-field brightness uniformity. Herein, I1,...,I5 represent diffracted light energies, with intensity decreasing along the light propagation direction.

3 Simulation

This study builds a simulation model based on the aforementioned influence of diffraction efficiency on uniformity. The simulation model employs a waveguide with dimensions of 60 mm × 40 mm, while the in-coupling region is set to 25 mm × 8 mm. The light source configuration matches the experimental setup, with a size of 12.3 mm × 9.2 mm. The non-grating modulation region is established within a 30 mm × 20 mm out-coupling grating area. The waveguide structure is illustrated in Figure 3(a). Due to constraints such as discontinuous exit pupils and eyebox size, the widths of the non-grating and grating regions in each modulation zone of the out-coupling area must be determined collectively by factors such as the field of view (FOV), exit pupil size, waveguide thickness, and glass material. The simulation model in this study adopts a 1 mm thick waveguide, with an in-coupling grating thickness of 4 μm and an out-coupling grating thickness of 3 μm. The lateral grating period is 420 nm, and the diagonal FOV is 40°. The model uses a single green light source with a wavelength of 530 nm.

Given the typical human pupil diameter of 3‑4 mm, the sub-period is set to 3 mm. The optimized waveguide model is shown in Figure 3(b), where the out-coupling grating region is divided into 10 zones with a period of 3 mm. In each zone, the non-grating region is located closer to the in-coupling grating side, while the grating region widths for the ten zones are 0.6 mm, 0.8 mm, 1 mm, 1.3 mm, 1.7 mm, 1.7 mm, 2.2 mm, 2.2 mm, 2.2 mm, and 2.6 mm, respectively. Measurements were conducted for both the pre-optimized and post-optimized waveguide models, as shown in Figures 3(c) and 3(d), which display the relative illuminance distribution of the out-coupling region before and after optimization, respectively. The results demonstrate that the exit pupil uniformity of the optimized structure is significantly improved.

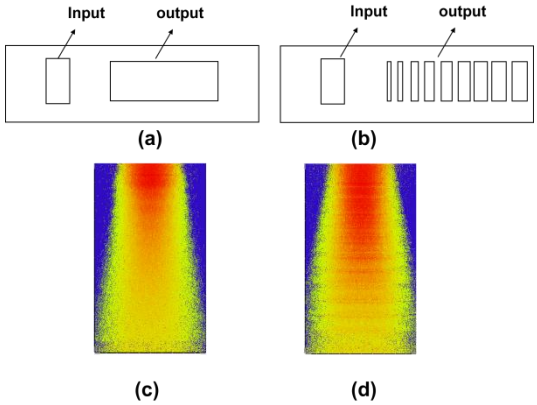

Fig.3 (a) Waveguide structure before optimization, (b) Waveguide structure after optimization, (c) Irradiance distribution of the out-coupling region before optimization ,(d) Irradiance distribution of the out-coupling region after optimization.

In this study, the exit pupil is equally divided into nine regions, and the average exit light intensity in each region is calculated. The brightness uniformity U_{FOV} of the exit pupil regions, serving as a relative reference for brightness uniformity, is given by the following equation:

$$U_{FOV} = \frac{1}{9} \times \sum_{i}^{9} \left(\frac{I(i)_{min}}{I(i)_{max}}\right), (i = 1,2, \ldots, 9) \qquad (3.1)$$

Here, i denotes the i-th measurement point, while $I(i)_{min}$ and $I(i)_{max}$ represent the minimum and maximum illuminance at the i-th point, respectively. From the table, it can be observed that the optimized structure achieves a uniformity of 42.92%, which is approximately twice as high as that of the pre-optimized structure.

Table 1 Irradiance and FOV uniformity before and after optimization.

	I_{max}-origin	I_{min}-origin	I_{max}-optimize	I_{min}-optimize
1	18.98	5.594	35.3	15.21
2	19.72	4.86	35.24	15.36
3	19.09	5.029	37.57	16.23
4	18.31	4.687	30.53	12.23
5	18.93	4.752	32.06	13.58
6	18.37	4.845	30.66	12.53
7	16.17	3.603	29.95	12.65
8	16.7	3.464	31.01	13.67
9	16.14	3.788	31.85	13.04
U_{FOV}	24.42%		**42.92%**	

4 Experiment

The flowchart of zonal efficiency-regulated PVG is shown in Fig. 4(a). The process includes: coating an alignment layer solution on the waveguide medium, placing it in the optical path for holographic interference exposure, spin-coating liquid crystal solution, UV curing, and finally ablating non-grating regions by laser based on simulation results to achieve zonal regulation of diffraction efficiency for the out-coupler grating.

The fabricated waveguide in Fig. 4(b) consists of an input coupler grating and an efficiency-regulated out-coupler grating from top to bottom.

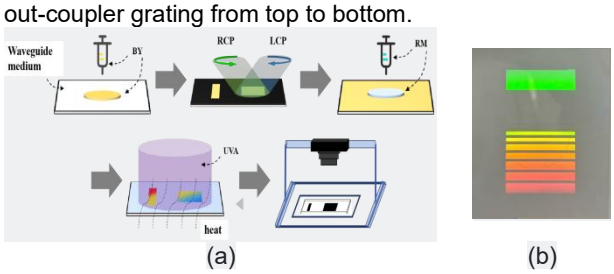

Fig. 4(a) Flowchart of zonal efficiency regulation fabrication, (b) Appearance of the fabricated waveguide.

The imaging performance of the waveguide display system is shown in Figs. 5(b)-(e). Given the typical human pupil diameter of 3-4 mm, experiments were conducted by simulating a human eye (4 mm) at 18 mm above the waveguide, with the experimental position schematically illustrated in Fig. 5(a). Comparison of imaging effects before and after efficiency regulation in different exit pupil regions confirms that this method enhances the brightness uniformity of the waveguide imaging system.

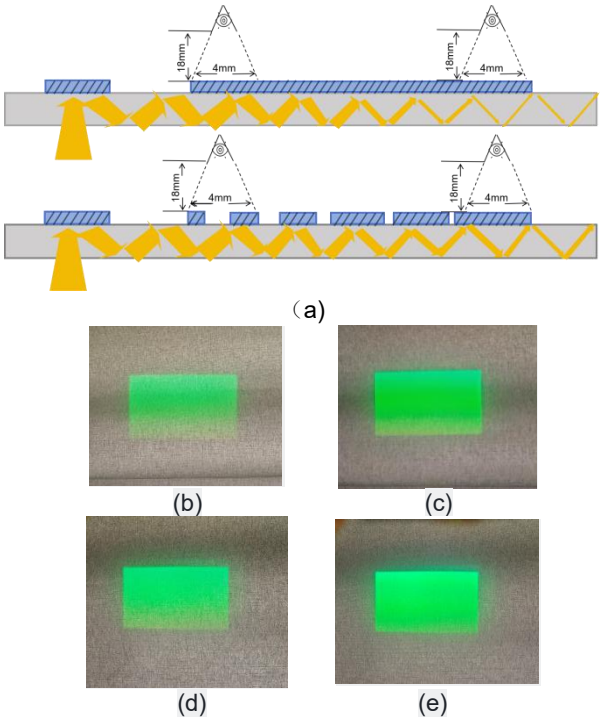

Fig. 5(a) Schematic of experimental position; (b) Imaging effect with uniform out-coupling diffraction efficiency in high-intensity region; (c) Imaging effect with zonal-regulated out-coupling diffraction efficiency in high-intensity region;(d) Imaging effect with uniform out-coupling diffraction efficiency in low-intensity region; (e) Imaging effect with zonal-regulated out-coupling diffraction efficiency in low-intensity region.

5 Conclusions

This paper proposes a novel fabrication method for zonal efficiency-regulated PVG. By enabling light diffraction in grating regions and total internal reflection in non-grating regions, gradient regulation of blank areas in PVG out-couplers is achieved. Simulations show approximately 50% improvement in field-of-view uniformity, and experiments confirm enhanced exit pupil uniformity across different PVG regions. Moreover, this method addresses the zonal processing challenges of traditional techniques such as nanoimprinting and holds potential for improving the modulation transfer function (MTF).

Acknowledgements

This work was supported in part by the National Natural Science Foundation of China under Grants No.62105060,and in part by the Basic Research Program of Jiangsu Province under Grants BK20232040.

References

[1] Xiong, J., Hsiang, E.-L., He, Z., Zhan, T. & Wu, S.-T. Augmented reality and virtual reality displays: emerging technologies and future perspectives.

Light Sci Appl 10, 216 (2021).
[2] Xiong, J., Yin, K., Li, K. & Wu, S.-T. Holographic Optical Elements for Augmented Reality: Principles, Present Status, and Future Perspectives. Advanced Photonics Research 2, 2000049 (2021).
[3] Yishi W, Daming X, Yuning Z, Xiaohua L, and Shin-Tson W, Polarization volume grating with high efficiency and large diffraction angle, Opt. Express 24, 17746-17759 (2016).
[4] Yishi W, Yuning Z, Wei W, Yuchen G, Chuang W, Ran W, Lixuan Z, and Baoping W, High-efficiency and compact two-dimensional exit pupil expansion design for diffractive waveguide based on polarization volume grating, Opt. Express 31, 6601-6614 (2023).
[5] Ding, Y., Yang, Q., Yang, Z., Huang, Y. & Wu, S.-T. Breaking in-coupling efficiency and uniformity tradeoff in waveguide-based AR displays with polarization volume gratings. in Advances in Display Technologies XV (eds. Lee, J.-H. & Wang, Q.-H.) 5 (SPIE, San Francisco, United States, 2025).
[6] Lee, Y.H., He, Z. & Wu, S.-T. Optical properties of reflective liquid crystal polarization volume gratings. J. Opt. Soc. Am. B 36, D9 (2019).
[7] Hui Y., Chengfeng W., Jiacheng W.&Haifeng L., Design of Large-Angle Uniform Diffraction Metasurface Gratings for Augmented Reality Display. Acta Optica Sinica 45, 1105001 (2025).
[8] Lub, J., Broer, D. J., Wegh, R. T., Peeters, E. & I Van Der Zande, B. M. Formation of Optical Films by Photo-Polymerisation of Liquid Crystalline Acrylates and Application of These Films in Liquid Crystal Display Technology. Molecular Crystals and Liquid Crystals 429, 77–99 (2005).